Temperature-Independent Catalytic Two-Electron Reduction of Dioxygen by Ferrocenes with a Copper(II) Tris[2-(2-pyridyl)ethyl]amine Catalyst in the Presence of Perchloric Acid

Dipanwita Das,[†] Yong-Min Lee,[†] Kei Ohkubo,[‡] Wonwoo Nam,*[,†] Kenneth D. Karlin,*[,†,§] and Shunichi Fukuzumi*[,†,‡]

[†]Department of Bioinspired Science, Ewha Womans University, Seoul 120-750, Korea

[‡]Department of Material and Life Science, Division of Advanced Science and Biotechnology, Graduate School of Engineering, ALCA (JST), Osaka University, Suita, Osaka 565-0871, Japan

[§]Department of Chemistry, The Johns Hopkins University, Baltimore, Maryland 21218, United States

Ⓢ *Supporting Information*

ABSTRACT: Selective two-electron plus two-proton ($2e^-/2H^+$) reduction of O_2 to hydrogen peroxide by ferrocene (Fc) or 1,1′-dimethylferrocene (Me$_2$Fc) in the presence of perchloric acid is catalyzed efficiently by a mononuclear copper(II) complex, $[Cu^{II}(tepa)]^{2+}$ (**1**; tepa = tris[2-(2-pyridyl)ethyl]-amine) in acetone. The $E_{1/2}$ value for $[Cu^{II}(tepa)]^{2+}$ as measured by cyclic voltammetry is 0.07 V vs Fc/Fc$^+$ in acetone, being significantly positive, which makes it possible to use relatively weak one-electron reductants such as Fc and Me$_2$Fc for the overall two-electron reduction of O_2. Fast electron transfer from Fc or Me$_2$Fc to **1** affords the corresponding Cu^I complex $[Cu^I(tepa)]^+$ (**2**), which reacts at low temperature (193 K) with O_2, however only in the presence of HClO$_4$, to afford the hydroperoxo complex $[Cu^{II}(tepa)(OOH)]^+$ (**3**). A detailed kinetic study on the homogeneous catalytic system reveals the rate-determining step to be the O_2-binding process in the presence of HClO$_4$ at lower temperature as well as at room temperature. The O_2-binding kinetics in the presence of HClO$_4$ were studied, demonstrating that the rate of formation of the hydroperoxo complex **3** as well as the overall catalytic reaction remained virtually the same with changing temperature. The apparent lack of activation energy for the catalytic two-electron reduction of O_2 is shown to result from the existence of a pre-equilibrium between **2** and O_2 prior to the formation of the hydroperoxo complex **3**. No further reduction of $[Cu^{II}(tepa)(OOH)]^+$ (**3**) by Fc or Me$_2$Fc occurred, and instead **3** is protonated by HClO$_4$ to yield H$_2$O$_2$ accompanied by regeneration of **1**, thus completing the catalytic cycle for the two-electron reduction of O_2 by Fc or Me$_2$Fc.
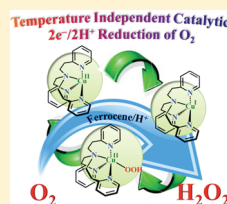
■ INTRODUCTION

Among copper proteins containing one or more copper ions as active site prosthetic groups, many are involved in dioxygen (O_2) processing and they can be classified into several types depending on their function and their specific copper ion coordination environments.[1,2] Suitable ligation of the reduced form Cu^I complexes includes N-, S-, or O-atom donor elements, which at some point in the protein catalytic cycle allows for reaction with O_2 to generate copper−O_2 complexes, $Cu^{II}_n(O_2)$ (n = typically 1−3), which are utilized for O_2 transport ($2Cu^I + O_2 \leftrightarrow Cu_2(O_2)$) and substrate oxygenation.[1−4] Galactose oxidases[5] and amine oxidases,[6] which are one class of copper oxidases, catalyze two-electron substrate oxidations, while reducing O_2 to hydrogen peroxide (H_2O_2).[7] Multicopper oxidases such as laccase also activate oxygen at a site containing a 3 + 1 arrangement of four Cu atoms, exhibiting remarkable electroactivity for the four-electron reduction of oxygen at potentials approaching the thermodynamic value of 1.2 V (vs RHE).[8] Cytochrome *c* oxidases (C*c*Os), with a bimetallic active site consisting of a heme *a* and Cu (Fe$_{a3}$/Cu$_B$) are also capable of catalyzing the four-electron reduction of dioxygen to water while coupling this process to

membrane proton translocation and evenually to ATP biosynthesis.[9,10]

The catalytic four-electron reduction of dioxygen (O_2) to water has merited increasing attention not only because it aids the elucidation of fundamental principles relevant to biological processes (as above) but also because of the technological significance, such as in fuel cell applications.[11−18] In the fuel cell, the four-electron reduction of O_2 is catalyzed at the cathode by platinum impregnated in carbon.[19,20] The high loadings of this precious metal that are required to achieve appreciable activity have prompted considerable activity in the development of catalysts based on nonprecious metals such as Co, Cu, and Fe.[21−27]

The catalytic two-electron reduction of O_2 to H_2O_2 has also attracted considerable interest, because H_2O_2 has been regarded as a promising candidate as a sustainable and clean energy carrier.[28−30] The free enthalpy change of the decomposition of hydrogen peroxide producing H_2O and O_2 is as large as −211 kJ mol^{-1}.[31] H_2O_2 has also been used as a highly efficient and environmentally benign oxidant in terms of

delignification efficiency and the reduction of negative ecological impacts.[32,33]

With regard to copper complex catalysts for O_2 reduction,[17] two mononuclear copper complexes having tmpa or BzPY1 ligands (tmpa = tris(2-pyridylmethyl)amine,[24a] BzPY1 = *N,N*-bis[(2-(2-pyridyl)ethyl]benzylamine][24b]) and one dinuclear copper complex with an N3 ligand (N3 = −(CH$_2$)$_3$-linked bis[(2-(2-pyridyl)ethyl)amine])[24b] (Scheme 1) have so far

Scheme 1
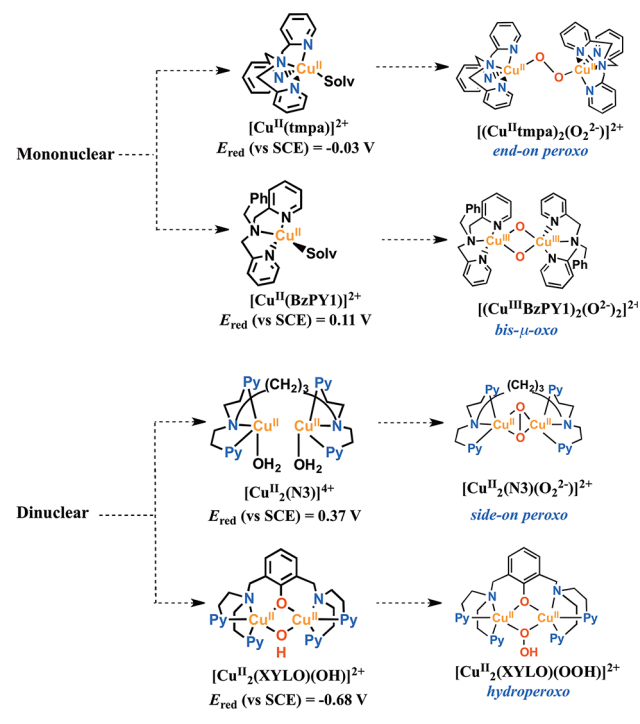
been found to efficiently catalyze the four-electron reduction of O_2 via the formation of $[\{(tmpa)Cu^{II}\}_2(\mu\text{-}1,2\text{-}O_2{}^{2-})]^{2+}$, $[Cu^{III}_2(BzPY1)(\mu\text{-}O^{2-})_2]^{2+}$, and $[Cu^{II}_2(N3)(\mu\text{-}\eta^2{:}\eta^2\text{-}O_2{}^{2-})]^{2+}$ intermediates, respectively. These Cu−O_2 complexes were prone to reductive O−O bond cleavage with protons to give water, in preference to the protonation leading to H_2O_2.[24] In contrast, the binuclear Cu(II) complex $[Cu^{II}_2(XYLO)(OH)]^{2+}$ (Scheme 1) (where XYLO is an *m*-xylene-linked bis(2-(2-pyridyl)ethyl)amine dinucleating ligand with a copper-bridging phenolate moiety) has been reported to catalyze the two-electron reduction of O_2 in the presence of trifluoroacetic acid via a hydroperoxo intermediate.[26] In all of these cases, however, a strong one-electron reductant such as decamethylferrocene (Fc*) was required to reduce O_2 with these Cu complex catalysts. In order to use weaker reductants, the one-electron reduction potentials of Cu^{II} complexes should be more positive than those found for $[Cu^{II}_2(XYLO)(OH)]^{2+}$ (−1.04 V vs Fc/Fc$^+$).[26] However, Cu^I complexes with rather positive one-electron-oxidation potentials cannot react with O_2, as reported previously.[34] Thus, there has so far been no report on the selective two- or four-electron reduction of O_2 by one-electron reductants weaker than Fc* with Cu complexes.

We report herein the selective two-electron reduction of O_2 by ferrocene (Fc) and 1,1′-dimethylferrocene (Me$_2$Fc), which are much weaker one-electron reductants than Fc*, using a mononuclear copper(II) complex, $[Cu^{II}(tepa)]^{2+}$ (**1**; tepa = tris[2-(2-pyridyl)ethyl]amine) in the presence of HClO$_4$ in

acetone. This behavior is in sharp contrast to that observed for the analogous complex $[Cu^{II}(tmpa)]^{2+}$ (tmpa = tris[2-(2-pyridyl)methyl]amine), which catalyzes the four-electron reduction of O_2 to water rather than the two-electron reduction of O_2 to H_2O_2 in the presence of HClO$_4$ in acetone; there, a strong one-electron reductant was required.[24a] Thus, a difference of an additional −CH$_2$− (methylene group) in the pyridylalkyl moiety of the ligand for Cu^{II}, N(CH$_2$CH$_2$-py)$_2$ vs N(CH$_2$-py)$_2$ (py = 2-pyridyl), results in (i) a remarkable difference in terms of the number of electrons by which moleclular oxygen is reduced (two electrons vs four electrons) and (ii) the reducing ability of one-electron reductants that can be employed to reduce O_2. More surprisingly, the rate of catalytic two-electron reduction of O_2 by Me$_2$Fc with **1** exhibits no temperature dependence. However, our study and analysis of the seemingly bizarre results suggesting there is no apparent activation energy for the catalytic reduction of O_2 can in fact be well understood. We have done this by clarifying the catalytic mechanism based on kinetic analyses as well as detection of the reactive intermediates involved in the catalytic cycle.

■ EXPERIMENTAL SECTION

Materials. Reagent grade quality solvents and chemicals were obtained commercially and used without further purification unless otherwise noted. 1,1′-Dimethylferrocene (Me$_2$Fc), ferrocene (Fc), hydrogen peroxide (30%), and HClO$_4$ (70%) were purchased from Aldrich Chemical Co. (U.S.), and NaI (99.5%) was from Junsei Chemical Co. (Japan). Acetone was purchased from JT Baker (U.S.) and used without further purification for non-air-sensitive experiments. For air-sensitive experiments, acetone was dried and distilled under argon and then deoxygenated by bubbling with argon for 30−45 min and kept over activated molecular sieves (4 Å) in a glovebox.[35] Preparation and handling of air-sensitive compounds were performed under an Ar atmosphere (<1 ppm O_2, <1 ppm H_2O) in a glovebox (Korea Kiyon Co., Ltd.). The copper complex $[Cu^{II}(tepa)](ClO_4)_2$ (**1**; tepa = tris(2-(2-pyridyl)ethylamine)[34] was prepared according to the literature procedure.[36]

Instrumentation. UV−vis spectra were recorded on a Hewlett-Packard 8453 diode array spectrophotometer equipped with a UNISOKU Scientific Instruments Cryostat USP-203A for low-temperature experiments or an UNISOKU RSP-601 stopped-flow spectrometer equipped with an MOS-type highly sensitive photodiode array. Cyclic voltammetry (CV) and differential pulse voltammetry (DPV) measurements were performed on an ALS 630B electrochemical analyzer, and voltammograms were measured in deaerated acetone containing 0.10 M tetra-*n*-butylammonium hexafluorophosphate (TBAPF$_6$) as the supporting electrolyte at room temperature. A conventional three-electrode cell was used with a glassy-carbon working electrode (surface area of 0.3 mm^2), and a platinum wire was the counter electrode. The glassy-carbon working electrode was routinely polished with a BAS polishing alumina suspension and rinsed with acetone before use. The potentials were measured with respect to the Ag/AgNO$_3$ (10 mM) reference electrode and were converted to values vs ferrocene/ferrocenium ion (Fc/Fc$^+$). All electrochemical measurements were carried out under atmospheric nitrogen pressure. X-band EPR spectra were recorded at 77 K using a JEOL JES-RE1XE spectrometer. The magnitude of modulation was chosen to optimize the resolution and signal-to-noise (S/N) ratio of the observed spectra under nonsaturating microwave power conditions. The g values and hyperfine coupling constants were calibrated using an Mn^{2+} marker. The experimental parameters for EPR spectra were as follows: microwave frequency 9.2 GHz, microwave power 1.0 mW, and modulation frequency 100 kHz. The EPR parameters were determined by anisotropic simulation using an AniSimu/FA version 2.0.0 program coded by JEOL Ltd.

Kinetic Measurements. Spectral changes in the UV−visible range were recorded on a Hewlett-Packard 8453 diode array spectropho-

tometer equipped with a Unisoku thermostated cell holder for low-temperature experiments. Rate constants for oxidation reactions of ferrocene derivatives by O_2 in the presence of catalytic amounts of $[Cu^{II}(tepa)]^{2+}$ and an excess amount of perchloric acid ($HClO_4$) in acetone at 298 K were determined by monitoring the appearance of the absorption band due to the corresponding ferrocenium ions (Fc^+, λ_{max} 620 nm, $\varepsilon_{max} = 430 \pm 20$ M^{-1} cm^{-1}; Me_2Fc^+, λ_{max} 650 nm, $\varepsilon_{max} = 360 \pm 20$ M^{-1} cm^{-1}). The limiting concentration of O_2 in an acetone solution was prepared by a mixed gas flow of O_2 and Ar. The mix of gas controlled by using a gas mixer (SMTEK, Korea), which could mix O_2 and Ar gases at specific pressures and flow rates. The O_2 concentration in an O_2-saturated acetone solution (11 mM) was previously determined by spectroscopic titration in the photooxidation of 10-methyl-9,10-dihydroacridine by O_2.[37]

Spectroscopic Measurements. The amount of H_2O_2 produced in reactions was determined by titration with iodide ion.[38] The diluted acetone solution of the reduced product of O_2 was treated with an excess of NaI. The amount of I_3^- formed was then quantified using its visible spectrum ($\lambda_{max} = 365$ nm, $\varepsilon = (2.5 \pm 0.1) \times 10^4$ M^{-1} cm^{-1}).

Low-Temperature Measurements. Under an open atmosphere, $[Cu^{II}(tepa)](ClO_4)_2$ (**1**; 0.16×10^{-3} M) was dissolved in 3 mL of O_2-free acetone. The cuvet was cooled to -80 °C in a Hewlett-Packard 8453 diode array spectrophotometer equipped with an Unisoku thermostated cell holder. $HClO_4$ (3.0×10^{-3} M) was added to the reaction solution, and the formation of the hydroperoxo species was followed by the change in the absorbance at 345 nm ($\varepsilon = 7000 \pm 100$ M^{-1} cm^{-1} determined for $[Cu^{II}(tepa)(OOH)]^+$.

■ RESULTS AND DISCUSSION

Electrocatalytic Reduction of O_2 with $[Cu^{II}(tepa)]$-$(ClO_4)_2$ (1) in the Presence of $HClO_4$. A cyclic voltammogram (CV) of **1** in deaerated acetone containing $TBAPF_6$ (0.10 M) at 298 K is shown in Figure 1. A quasi-reversible couple
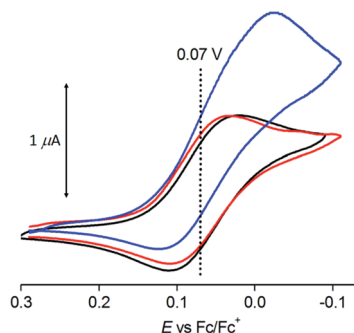
Figure 1. Cyclic voltammograms of **1** (1.0 mM) in deaerated (black line) and O_2-saturated (red line) acetone in the absence of $HClO_4$ and in the presence of $HClO_4$ (0.10 M) in O_2-saturated acetone (blue line) at 298 K. Working and counter electrodes were a glassy-carbon electrode and a Pt wire, respectively. $TBAPF_6$ (0.10 M) was used as the electrolyte. The sweep rate was 1.0 mV s^{-1}.

between the Cu^{II} and Cu^{I} forms of the complex is observed. From the $E_{1/2}$ values, the one-electron-reduction potential (E_{red}) of **1** was determined to be 0.07 ± 0.01 V (vs Fc/Fc^+) (Figure 1, black line). The longer-armed tepa ligand, as compared to that observed in the tmpa ligand (Chart 1), leads to complex **1** with coordination of a solvent (L) that is nearly perfectly square-based pyramidal in structure, resulting in nearly a 0.5 V more positive shift of E_{red} as compared with that of $[Cu^{II}(tmpa)]^{2+}$ (**A**) (E_{red} vs $Fc/Fc^+ = -0.40$ V).[24a] The tepa ligand forms a six-membered chelate ring in **1**, whereas the tmpa ligand forms only a five-membered chelate ring in $[Cu^{II}(tmpa)]^{2+}$ (Chart 1). Such a change from the five- to the six-membered ring is generally known to result in a large

Chart 1

$[Cu^{II}(tmpa)L]^{2+}$ $[Cu^{II}(tepa)L]^{2+}$
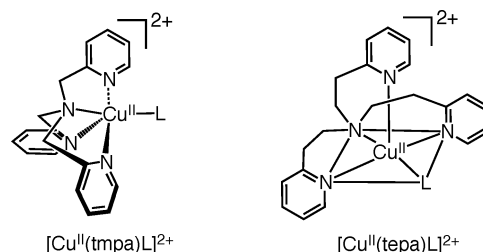
positive shift in the $Cu^{II/I}$ redox potential.[39] This effect has its origin in the difference in ligand binding constants to Cu(II), which are much larger for five- vs six-membered chelate rings in multidentate ligands, as elucidated and summarized by Rorabacher and co-workers.[39c,d]

The redox wave of the $Cu^{II/I}$ couple of **1** without $HClO_4$ in the presence of O_2 (red line in Figure 1) remains the same as that in the absence of O_2 (black line in Figure 1). In the presence of both O_2 and $HClO_4$, however, a catalytic cathodic current is observed (blue line in Figure 1), indicating that O_2 can be reduced catalytically by **1** in the presence of $HClO_4$ in acetone. A slow sweep rate (1.0 mV s^{-1}) is required to observed the catalytic cathodic current, indicating that the catalysis is a relatively slow process (vide infra).

Catalytic Two-Electron Reduction of O_2 by Me_2Fc and Fc with 1 in the Presence of $HClO_4$. The addition of a catalytic amount of **1** to an acetone solution of Fc/Me_2Fc containing O_2 ($[O_2] = 2.2$ mM) and perchloric acid ($HClO_4$) results in efficient dioxygen reduction to afford the corresponding ferrocenium/dimethylferrocenium cation (Fc^+/Me_2Fc^+), as shown in Figure 2 (see also Figure S1 in the Supporting
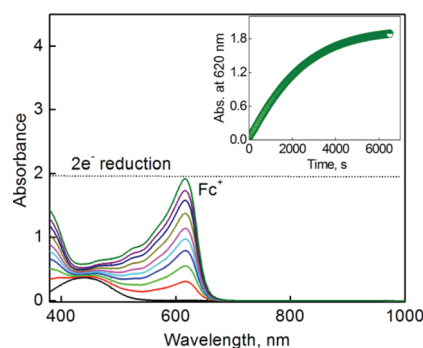
Figure 2. UV−vis spectral changes observed in the two-electron reduction of O_2 (2.2 mM) by Fc (10 mM) with $HClO_4$ (40 mM) catalyzed by **1** (0.040 mM) in acetone at 298 K. The inset shows the time profile of the absorbance at 620 nm due to Fc^+.

Information), where 2 equiv of Fc^+ ($\lambda_{max} = 620$ nm) or Me_2Fc^+ ($\lambda_{max} = 650$ nm), relative to the number of mol equiv of O_2, was formed in the presence of excess $HClO_4$. Thus, the stoichiometry of the catalytic oxidation of Fc and Me_2Fc by O_2 is given by eq 1. The formation of H_2O_2 was confirmed by

$$2Fc + O_2 + 2H^+ \rightarrow 2Fc^+ + H_2O_2 \qquad (1)$$
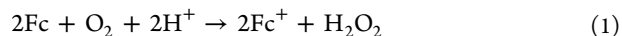
iodometric titration (Figure S2a in the Supporting Information). The amount of I_3^- produced ($\lambda_{max} = 365$ nm) was the same as that produced by the reaction of the stoichiometric

amount of H_2O_2 with I^- (Figure S2b in the Supporting Information).

The rate of formation of Fc^+ and Me_2Fc^+ obeyed pseudo-first-order kinetics under the conditions $[1] \ll [O_2] \ll [Me_2Fc] \ll [HClO_4]$ (Figure 2 inset; Figure S1 inset in the Supporting Information). Because 2 equiv of Fc^+ is formed in the reduction of O_2 (eq 1), the pseudo-first-order kinetics of formation of Fc^+ are given by eq 2, where the initial

$$d[Fc^+]/dt = k_{obs}[[Fc^+]_f - [Fc^+]] = k_{obs}[O_2] \qquad (2)$$

concentration of O_2 ($[O_2]_0$) is equal to 2 times the final concentration of Fc^+ ($2[Fc^+]_f$); $[Fc^+] = 2\{[O_2]_0 - [O_2]\}$. The time profiles of the absorbance at 620 nm due to Fc^+ and at 650 nm due to Me_2Fc^+ and the first-order plots by varying catalyst (Figure 3a; see also Figures S4a and S5a,b in the Supporting
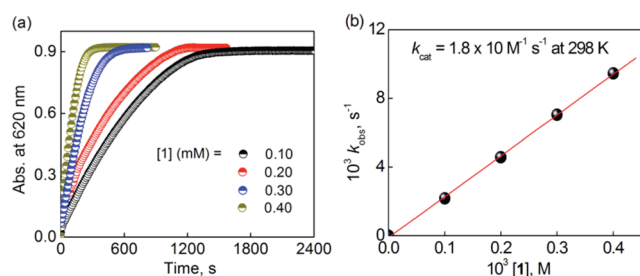
Figure 3. (a) Time profiles of the absorbance at 620 nm due to Fc^+ in the two-electron reduction of O_2 ($[O_2]$ = 1.0 mM) catalyzed by **1** (0.10 mM (black), 0.20 mM (red), 0.30 mM (blue), and 0.40 mM (dark yellow)) with Fc (10 mM) in the presence of $HClO_4$ (60 mM) in acetone solution at 298 K. (b) Plot of k_{obs} versus [**1**] for the two-electron reduction of O_2 ($[O_2]$ = 1.0 mM) catalyzed by **1** with Fc (10 mM) in the presence of $HClO_4$ (60 mM) in acetone at 298 K.

Information), $HClO_4$ (Figures S3a, S4b, and S5c,d in the Supporting Information), O_2 (Figures S3c, S4c, and S6a,b in the Supporting Information) and the electron donors Fc (Figures S3b and S4d in the Supporting Information) and Me_2Fc (Figures S6c,d in the Supporting Information) are shown as indicated. The pseudo-first-order rate constant (k_{obs}) increased linearly with an increasing concentration of **1** (Figure 3b; Figure S7a in the Supporting Information) and $HClO_4$ (Figure 4a; Figure S7b in the Supporting Information), whereas the k_{obs} value remained the same with an increasing concentration of O_2 (Figures S3d and S7c in the Supporting
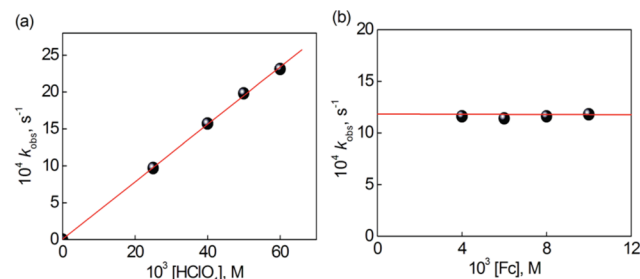

Figure 4. (a) Plot of k_{obs} versus $[HClO_4]$ for the two-electron reduction of O_2 by Fc (10 mM) catalyzed by **1** (0.10 mM) in an acetone solution containing O_2 (1.0 mM) at 298 K. (b) Plot of k_{obs} versus [Fc] for the two-electron reduction of O_2 catalyzed by **1** (0.10 mM) with Fc in the presence of $HClO_4$ (30 mM) in an acetone solution containing O_2 ($[O_2]$ = 1.0 mM) at 298 K.

Information; note that the reaction rate is already first order with respect to $[O_2]$, cf. eq 2), Fc (Figure 4b), and Me_2Fc (Figures S7d in the Supporting Information). Thus, the overall rate expression is given by eq 3, where k_{cat} is the apparent third-

$$d[Fc^+]/dt = k_{cat}[1][O_2][H^+] \qquad (3)$$

order rate constant for the catalytic two-electron reduction of O_2 by Fc and Me_2Fc. The kinetic formulation in eq 3 obtained in this study is quite unique because the rate is proportional to concentrations of not only the catalyst **1** but also O_2 and $HClO_4$. In such a case, the rate-determining step in the catalytic cycle should involve the reactions of **1** with O_2 and H^+. In order to elucidate the catalytic mechanism that could explain such a unique kinetic formulation, we decided to examine each step in the catalytic cycle, step by step.

We also examined the overall catalytic reaction at different temperatures. Remarkably, variable-temperature studies revealed that the catalytic rate was not affected by changes in temperature (Figure 5).
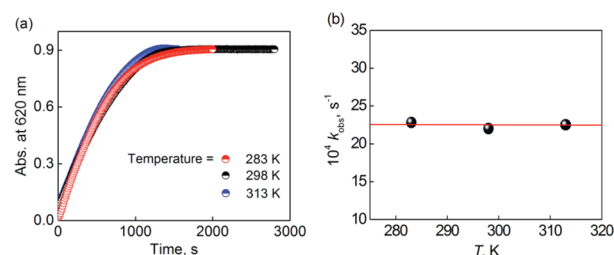
Figure 5. (a) Time profiles of the absorbance at 620 nm due to Fc^+ in the two-electron reduction of O_2 (1.0 mM) catalyzed by **1** (0.10 mM) with Fc (10 mM) in the presence of $HClO_4$ (60 mM) in an acetone solution at variable temperatures (283 K (red), 298 K (black), and 313 K (blue)). (b) Plot of k_{obs} versus temperature (T) for the two-electron reduction of O_2 catalyzed by **1** (0.10 mM) with Fc (10 mM) in the presence of $HClO_4$ (60 mM) in an acetone solution with O_2 ($[O_2]$ = 1.0 mM) at different temperatures.

Electron Transfer from Ferrocene Derivatives to 1. Electron transfer from Fc and Me_2Fc (E_{ox} = 0.0 V and −0.11 V vs Fc/Fc$^+$)[40,41] to **1** (E_{red} = 0.07 V vs Fc/Fc$^+$, vide supra) occurs efficiently because the reactions are exergonic ($\Delta G_{et} < 0$). The rates of electron transfer from Fc or Me_2Fc to **1** were too fast to be determined at 298 K. Thus, these kinetics were determined at lower temperatures. The rate of formation of Fc^+ and Me_2Fc^+ obeyed pseudo-first-order kinetics in acetone at lower temperatures (see the time profiles in Figure 6a and in Figures S8a,c, S9a, S11a,c, and S12a,c in the Supporting Information; first-order plots in Figures S8b,d, S9b, S10a, S11b,d, and S12b,d in the Supporting Information). The observed pseudo-first-order rate constant (k_{obs}) increased linearly with increasing concentration of Fc and Me_2Fc (Figure 6b; see also Figures S10 and S13 in the Supporting Information). The second-order rate constant (k_{et}) for electron transfer from Fc to **1** was determined from the slope of a linear plot of k_{obs} versus [Fc]. The temperature dependence of k_{et} was examined (Figure S14 in the Supporting Information), and the second-order rate constants of electron transfer from Fc and Me_2Fc to **1** at 298 K were determined to be $(6.0 \pm 0.3) \times 10^4$ and $(6.1 \pm 0.3) \times 10^4$ M^{-1} s^{-1}, respectively, from extrapolations of the Eyring plots (Figure S14 in the Supporting Information). The k_{et} values for electron transfer from Fc or Me_2Fc to **1** are significantly larger
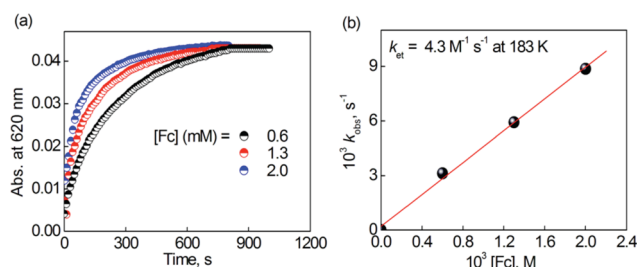
Figure 6. (a) Time profiles of the absorbance at 620 nm due to Fc$^+$ in the electron transfer reaction from Fc (0.60 mM (black), 1.3 mM (red), and 2.0 mM (blue)) to **1** (0.10 mM) in acetone at 183 K. (b) Plot of k_{obs} versus [Fc] in the electron transfer from Fc to [Cu^{II}(tepa)]$^{2+}$ (**1**; 0.10 mM) in acetone solution at 183 K.

than the corresponding $k_{obs}/[1]$ values (see eq 2) (18 ± 1 M^{-1} s^{-1} in Figure 3b for Fc and 17 ± 1 M^{-1} s^{-1} in Figure S7a (Supporting Information) for Me$_2$Fc). Thus, it has been confirmed that the electron-transfer step is not the rate-determining step in the catalytic cycle, being consistent with the kinetic equation (eq 2), where the k_{obs} values were independent of the concentrations of [Fc] and [Me$_2$Fc].

The Eyring plot (Figure S14 in the Supporting Information) affords the activation enthalpies ($\Delta H^{\ddagger}$ = 9.5 ± 0.2 and 9.2 ± 0.2 kcal mol^{-1}) and activation entropies ($\Delta S^{\ddagger}$ = −3 ± 2 and −2 ± 2 cal K^{-1} mol^{-1}) for the Fc and Me$_2$Fc reactions, respectively. An activation entropy close to 0 was previously reported for electron transfer from ferrocene derivatives to Cu(II) complexes.[26,42] The electron transfer from Fc and Me$_2$Fc to **1** results in formation of the Cu(I) complex [Cu^{I}(tepa)]$^+$ (**2**), which can reduce O$_2$ in the presence of HClO$_4$. Next we examined the reaction of [Cu^{I}(tepa)]$^+$ with O$_2$ in presence of HClO$_4$ at low temperatures to detect intermediates.

Detection of Intermediates in the Catalytic Two-Electron Reduction of O$_2$ by Fc with [Cu^{II}(tepa)]$^{2+}$ (1). When **1** was treated with O$_2$ and HClO$_4$, the bright green hydroperoxo complex **3** (vida infra) was produced, possessing an intense absorption band at 345 nm (ε = 7000 ± 100 M^{-1} cm^{-1}) corresponding to a LMCT band (HOO$^-$ → Cu), and a d−d transition envelope at 660 nm (ε = 160 ± 5 M^{-1} cm^{-1}) (Figure 7).
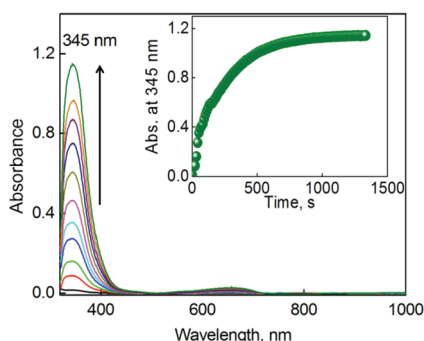
Figure 7. Formation of the hydroperoxo complex [Cu^{II}(tepa)-(OOH)]$^+$ (**3**; λ_{max} = 345 nm) in the reaction of [Cu^{I}(tepa)]$^+$ (0.16 mM) ([Cu^{I}(tepa)]$^+$ was generated from room-temperature mixing of [Cu^{II}(tepa)]$^{2+}$ (0.16 mM) with Fc (0.32 mM)) with O$_2$ (2.2 mM) in acetone at 193 K in the presence of HClO$_4$ (3.0 mM). The inset shows the time profile of the absorbance at 345 nm due to the generation of [Cu^{II}(tepa)(OOH)]$^+$ (**3**).

The stoichiometry of the O$_2$ binding step in the presence of HClO$_4$ was determined by a control reaction. When Fc was used exactly at the level of 1 equiv relative to [Cu^{II}(tepa)]$^{2+}$ (Figure S15 in the Supporting Information), the amount of **3** produced is about half judging from a comparison of the results in Figure 7 with those in Figure S15 (Supporting Information). Thus, the stoichiometry of formation of **3** from the copper(I) complex is: [Cu^{I}(tepa)]$^+$ + Fc + O$_2$ + H$^+$ → [Cu^{II}(tepa)-(OOH)]$^+$ + Fc$^+$ (**3**).

The formation of hydroperoxo complex was again checked by an alternative "authentic" method. Figure S16 (Supporting Information) shows the spectral change for the reaction of [Cu^{II}(tepa)]$^{2+}$ (**1**) and H$_2$O$_2$ (10 equiv) in acetone at 193 K in the presence of 2 equiv of Me$_4$NOH. The result is that the same absorption band at 345 nm (ε = 7000 ± 100 M^{-1} cm^{-1}) appears together with a d−d band at 660 nm (ε =160 ± 5 M^{-1} cm^{-1}) (see Figure S16 in the Supporting Information).

It should be noted here that Masuda, Kodera, Itoh, and their co-workers have reported on similar Cu(II)−hydroperoxo complexes with tridentate N$_3$ or tetradentate N$_4$ pyridylalkyl-amine ligands, such as the ligand bpba (bpba = bis(2-pyridylmethyl-*tert*-butylamine) which has a strong absorption band at 350 nm (ε = 3400 ± 100 M^{-1} cm^{-1}) and d−d bands at 564 nm (ε = 150 ± 5 M^{-1} cm^{-1}) and 790 nm (sh).[43] There were several other Cu(II)−hydroperoxo complexes reported hitherto having LMCT bands which lie in the highest energy region (380 nm for five-coordinate trigonal-bipyramidal [Cu(bppa)(OOH)]$^+$ where bppa = bis(6-pivalamido-2-pyridylmethyl)(2-pyridylmethyl)amine,[44] 357 nm for five-coordinate square-pyramidal [Cu(N$_3$S-type)(OOH)]$^+$ where N$_3$S = 2-bis(6-methyl-2-pyridylmethyl)amino-1-(phenylthio)-ethane,[45] 395 nm for five-coordinate [Cu$^{II}_2$(XYLO)(OOH)]$^{2+}$ where XYLO = 2,6-bis[bis[2-(2-pyridyl)ethyl]amino]-phenolate,[46] and 379 nm for five-coordinate [Cu^{II}(tmpa)-(OOH)]$^+$ where tmpa = tris(2-pyridylmethyl)amine[43,47]).

An EPR spectrum of [Cu^{II}(tepa)]$^{2+}$ in frozen acetone solution at 77 K exhibits the parameters $g_{\parallel}$ = 2.320 ± 0.002, $g_{\perp}$ = 2.128 ± 0.001 and |$A_{\parallel}$| = 159 ± 3 G, indicating the typical tetragonal spectrum for four lines in the downfield region due to the Cu nuclear spin ($I = ^3/_2$) (Figure 8a). The reaction of [Cu^{I}(tepa)]$^+$ (**2**), which was produced by the electron-transfer reduction of [Cu^{II}(tepa)]$^{2+}$ (**1**) by Me$_2$Fc, with O$_2$ in the presence of HClO$_4$ in acetone afforded an EPR spectrum at 77 K with EPR parameters of $g_{\parallel}$ = 2.259 ± 0.002, $g_{\perp}$ = 2.063 ± 0.001, and |$A_{\parallel}$| = 165 ± 3 G due to Cu with superhyperfine splitting due to three equivalent nitrogens (|$A(3N)_{\perp}$| = 14.3 ± 0.5 G) as shown in Figure 8b. This spectrum is clearly different from that of [Cu^{II}(tepa)]$^{2+}$ (see Figure 8a), whereas the same EPR spectrum was observed at 77 K for [Cu^{II}(tepa)OOH]$^+$, which was produced by the reaction of [Cu^{II}(tepa)]$^{2+}$ with H$_2$O$_2$ in the presence of Me$_4$NOH in acetone. The computer-simulated spectra of [Cu^{II}(tepa)]$^{2+}$ and [Cu^{II}(tepa)OOH]$^+$ with the EPR parameters described above agree perfectly with the observed spectra, as shown in Figure 8.[48]

A similar EPR spectrum was reported for [Cu(bpba)-(OOH)]$^+$ with EPR parameters of $g_{\parallel}$ = 2.26, $g_{\perp}$ = 2.06 and |$A_{\parallel}$| = 175 G in acetone at 77 K, although no superhyperfine due to nitrogens was observed in that case.[43] Thus, the EPR spectrum observed in Figure 8b and the LMCT band seen in the higher energy region in Figure 7 strongly suggest the formation of [Cu^{II}(tepa)OOH]$^+$ in the reaction of [Cu^{I}(tepa)]$^+$ with O$_2$ in the presence of HClO$_4$ in acetone.
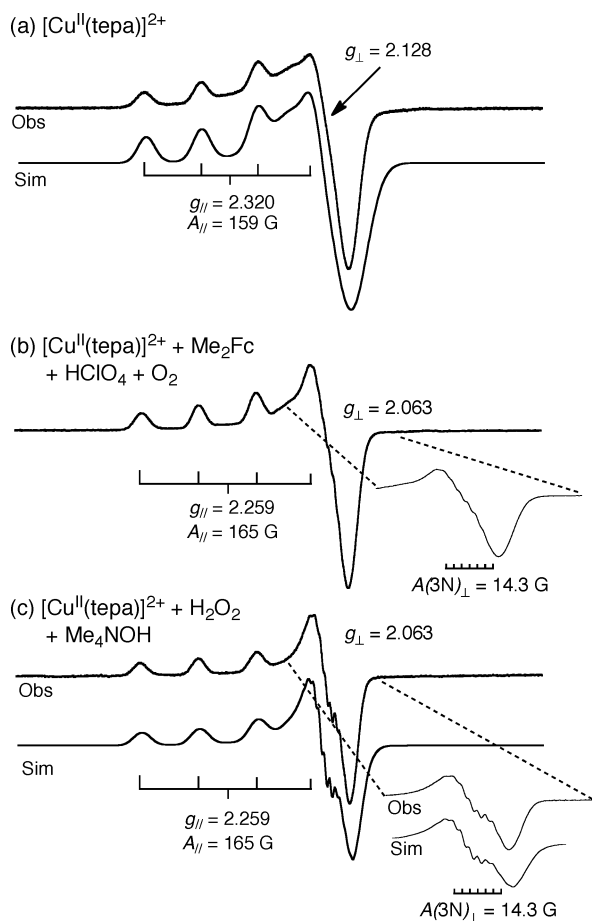
Figure 8. X-band EPR spectra of (a) $[Cu^{II}(tepa)]^{2+}$ (5.0×10^{-5} M) in deaerated acetone at 77 K, (b) the reaction solution of **1** (5.0×10^{-5} M) with Me_2Fc (3.0×10^{-4} M) in the presence of $HClO_4$ (3.0×10^{-3} M) in O_2-saturated acetone at 77 K, and (c) $[Cu^{II}(tepa)(OOH)]^+$ (**3**) generated by reaction of $[Cu^{II}(tepa)]^{2+}$ (5.0×10^{-5} M) with H_2O_2 (1.0×10^{-3} M) in the presence of Me_4NOH (1.0×10^{-3} M) recorded in deaerated acetone at 77 K. Experimental parameters: microwave frequency 9.2 GHz, microwave power 1.0 mW, and modulation frequency 100 kHz. The simulated spectra were obtained with the EPR parameters $g_\| = 2.320$, $g_\perp = 2.128$, $A_\| = 159$ G, $A_\perp = 25$ G, line width $\sigma_\|$ (σ_{zz}) = 48 G, and $\sigma_\perp = \sigma_{xx} = \sigma_{yy} = 100$ G for $[Cu^{II}(tepa)]^{2+}$ and $g_\| = 2.259$, $g_\perp = 2.063$, $A_\| = 165$ G, $A_\perp = 22$ G, line width $\sigma_\|$ (σ_{zz}) = 25 G, $\sigma_{xx} = 10$, and $\sigma_{yy} = 70$ G for Cu and 14.3 G for 3N of $[Cu^{II}(tepa)(OOH)]^+$.

$[Cu^I(tepa)]^+$ (**2**) was known to be unreactive toward O_2 in the absence of $HClO_4$.[34] This lack of reactivity likely results from a combination of steric hindrance and electronic effects and also from the complex's high positive redox potential. The crystal structures of $[Cu^{II}(tepa)]^{2+}$ (**1**) and $[Cu^I(tepa)]^+$ were reported earlier.[49,50] The structural parameters clearly indicate that both the complexes are strongly constrained. Because the arm size of the tepa ligand is larger than that of the tmpa ligand, any steric effects may be more prominent with tepa's six-membered chelate rings; the pyridyl rings of the donor ligands may extend out more into the region around the Cu^{II} ion, where a fifth ligand, such as hydroperoxide anion, would approach and bind the metal ion.

In another homologous set of structures, $[Cu^{II}(tepa)Cl]^+$ and $[Cu^{II}(tmpa)Cl]^+$, the Cu^{II}–Cl bond is also found to be lengthened in the tepa case by 0.056 Å.[39a] In fact, in all tepa vs tmpa Cu^{II} pentacoordinate structures, $[Cu^{II}(tepa)X]^{2+/+}$, the

anionic or neutral X ligand is in an equatorial position of an overall square-based-pyramidal structure, while the X ligand in $[Cu^{II}(tmpa)X]^{2+/+}$ structures is in an axial position of a nearly perfect trigonal-bipyramidal coordination environment.[34,39a] For $[Cu^{II}(tepa)OOH]^+$, due to (i) the hydroperoxo ligand position in the coordination environment, (ii) because of a likely elongated Cu–O bond, or (iii) both, cleavage by acid to produce H_2O_2 is preferred. This is in contrast to the O–O reductive cleavage which is observed for the intermediate $[Cu^{II}(tmpa)OOH]^+$ species likely formed during the four-electron, four-proton reduction of O_2 to water using $[Cu^{II}(tmpa)]^{2+}$ as catalyst (vide infra).[24a]

The rate of formation of $[Cu^{II}(tepa)OOH]^+$ at 193 K obeyed first-order kinetics (Figure 9a and Figure S17 in the Supporting
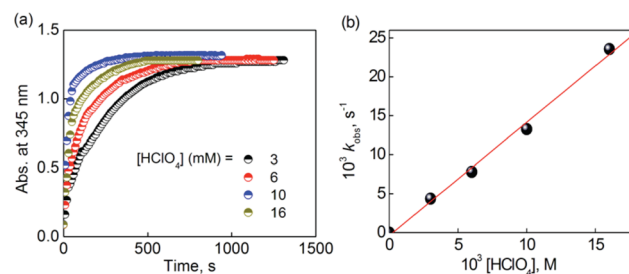
Figure 9. (a) Time profiles of the absorbance at 345 nm due to $[Cu^{II}(tepa)(OOH)]^+$ (**3**) in the O_2 (2.2 mM) binding step to $[Cu^I(tepa)]^+$ (0.18 mM) ($[Cu^I(tepa)]^+$ was produced from room-temperature mixing of $[Cu^{II}(tepa)]^{2+}$ (0.18 mM) with Fc (0.36 mM)) in the presence of various concentrations of $HClO_4$ (3 mM (black), 6 mM (red), 10 mM (blue), and 16 mM (dark yellow)) in an acetone solution at 193 K. (b) Plot of k_{obs} versus $[HClO_4]$ for the O_2 (2.2 mM) binding step to $[Cu^I(tepa)]^+$ (0.18 mM) in the presence of various concentrations of $HClO_4$.

Information), and the pseudo-first-order rate constant increased in proportion to the concentration of $HClO_4$ (Figure 9b). The observed rate constant exhibits no temperature dependence in the range between 193 and 223 K (Figure 10 and Figure S18 in the Supporting Information). The apparent zero activation energy or even negative activation energy has precedence and has been observed for reactions when an intermediate first forms and when the absolute value of the heat of formation of the indermediate is equal to or larger than the
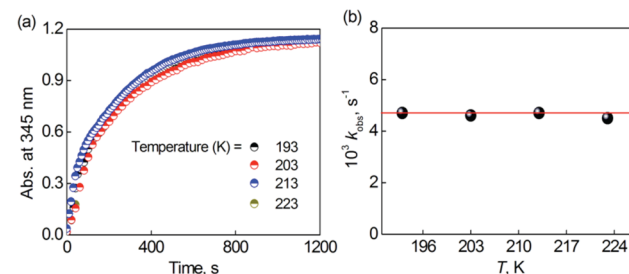
Figure 10. (a) Time profiles of the absorbance at 345 nm due to $[Cu^{II}(tepa)(OOH)]^+$ in the O_2 ($[O_2]$ = 2.2 mM) binding step in the presence of $HClO_4$ (3.0 mM) with $[Cu^I(tepa)]^+$ (0.16 mM) ($[Cu^I(tepa)]^+$ was produced from room-temperature mixing of $[Cu^{II}(tepa)]^{2+}$ (0.16 mM) with Fc (0.32 mM)) at different temperatures (193 K (black), 203 K (red), 213 K (blue), and 223 K (dark yellow)). (b) Plot of k_{obs} versus T (K) in the O_2 (2.2 mM) binding process to $[Cu^I(tepa)]^+$ (**2**) (0.16 mM) with $HClO_4$ (3.0 mM) in an acetone solution at variable temperatures.

activation enthalpy of the subsequent conversion of inter-mediate to the products, i.e., $-\Delta H \geq \Delta H^{\ddagger}$.[51−55] In the case of $[Cu^{I}(tmpa)]^{+}$, the reaction of $[Cu^{I}(tmpa)]^{+}$ with O_2 is known to produce the superoxo complex $[Cu^{II}(tmpa)(O_2^{\bullet-})]^{+}$. The ΔH and ΔS values were reported to be -11 kcal mol^{-1} and -23 cal K^{-1} mol^{-1}, respectively, when the ΔG value at 193 K is -6.7 kcal mol^{-1}.[56] This indicates that the formation of the superoxo complex is highly exergonic. The formation of $[Cu^{II}(tmpa)(O_2^{\bullet-})]^{+}$ is followed by the reduction with another molecule of $[Cu^{I}(tmpa)]^{+}$ to produce the dinuclear copper-(II)−-peroxo (end-on) complex.[56]

In the case of $[Cu^{I}(tepa)]^{+}$, neither a superoxo nor a peroxo complex has been observed by the reaction with O_2 at 193 K. Thus, the ΔG value of formation of the superoxo complex $[Cu^{II}(tepa)(O_2^{\bullet-})]^{+}$ must be positive. The activation barrier to access the superoxo complex in the absence of protons is too high. However, this does not necessarily mean that the ΔH value is also positive. If the ΔS value of formation of $[Cu^{II}(tepa)(O_2^{\bullet-})]^{+}$ is the same as that of $[Cu^{II}(tmpa)-(O_2^{\bullet-})]^{+}$, i.e., large and negative, the ΔG value becomes positive (endergonic, therefore no formation) when the ΔH value is more positive than -5.0 kcal mol^{-1}.

Thus, the ΔH value of formation of $[Cu^{II}(tepa)(O_2^{\bullet-})]^{+}$ could be negative enough to compensate for the $\Delta H^{\ddagger}$ value required for the subsequent PCET reduction to produce the peroxo complex $[Cu^{II}(tepa)OOH]^{+}$, formation of which was observed at 193 K, as shown in Figure 7. The energetics of formation of $[Cu^{II}(tepa)OOH]^{+}$ via the PCET reduction of $[Cu^{II}(tepa)(O_2^{\bullet-})]^{+}$ are shown in Scheme 2. If the $-\Delta H$ value

**Scheme 2**
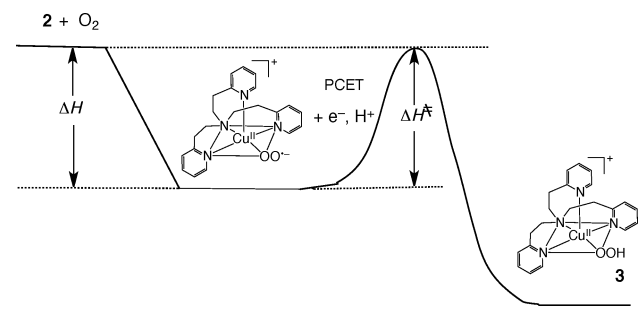
of formation of $[Cu^{II}(tepa)(O_2^{\bullet-})]^{+}$ happened to be equal or very close to the $\Delta H^{\ddagger}$ value of PCET reduction of $[Cu^{II}(tepa)(O_2^{\bullet-})]^{+}$ (Scheme 2), the formation rate of $[Cu^{II}(tepa)OOH]^{+}$ would be independent of temperature, as observed in this chemical system (see Figure 10 and Figure S18 in the Supporting Information).

No electron transfer from Fc or Me$_2$Fc to the hydroperoxo complex $[Cu^{II}(tepa)(OOH)]^{+}$ (**3**) occurs, as shown by the data in Figure 11a, where the absorption spectrum due to **3** remained constant by the addition of Fc or Me$_2$Fc. This is the reason the selective two-electron reduction of O_2 by Fc and Me$_2$Fc occurs; that is, the hydroperoxo−copper(II) complex **3** is not susceptible to reduction, and thus with catalyst and HClO$_4$ protonation occurs instead and H$_2$O$_2$ is produced.

When excess HClO$_4$ was further added to an acetone solution of $[Cu^{II}(tepa)(OOH)]^{+}$ (**3**) and Me$_2$Fc, the absorption band due to **3** disappeared without formation of Me$_2$Fc^{+} (Figure 11b), indicating that the protonation of **3** occurs to yield $[Cu^{II}(tepa)]^{2+}$ (**1**) and hydrogen peroxide;
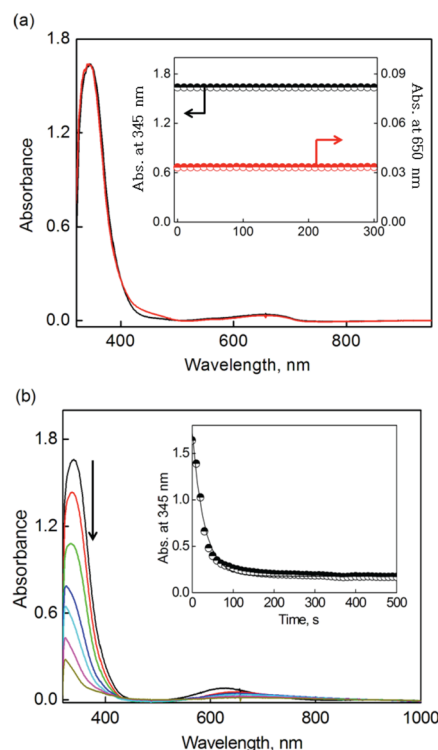
Figure 11. (a) UV−visible spectra of the hydroperoxo species $[Cu^{II}(tepa)(OOH)]^{+}$ (**3**; 0.23 mM) (black line) and **3** (0.23 mM) plus excess Me$_2$Fc (1.5 mM) (red line) in acetone at 193 K. (b) UV−visible spectral changes of **3** (0.23 mM) in the presence of HClO$_4$ (40 mM) in acetone at 193 K. The inset shows the time profile of the absorbance at 345 nm due to **3**.

reductive cleavage of peroxide occurs, even with the slightly stronger 1,1′-dimethylferrocene reductant.

We have also examined the temperature effect on this protonation step. Variable-temperature studies revealed that the rate of protonation of $[Cu^{II}(tepa)(OOH)]^{+}$ (**3**) became faster with increasing temperature (Figure S19 in the Supporting Information). The second-order rate constant (k_2) was estimated from an Eyring plot to be $(9.0 \pm 0.5) \times 10^2$ M^{-1} s^{-1} at 298 K, which is much larger than the $k_{obs}/[\mathbf{1}]$ values (vide supra). Thus, the protonation of hydroperoxo species is not the rate-determining step under the catalytic conditions.

The Eyring plot also afforded activation enthalpy ($\Delta H^{\ddagger} = 8.4 \pm 0.2$ kcal mol^{-1})[57] and activation entropy ($\Delta S^{\ddagger} = -16 \pm 0.5$ cal K^{-1} mol^{-1}) parameters for the copper−hydroperoxide protonation step.

Catalytic Mechanism. The catalytic mechanism of the two-electron reduction of O_2 by Me$_2$Fc and Fc with $[Cu^{II}(tepa)]^{2+}$ (**1**) in the presence of HClO$_4$ is summarized in Scheme 3. The initial electron transfer from Me$_2$Fc and Fc to **1** is fast, followed by the reaction of the copper(I) complex formed, $[Cu^{I}(tepa)]^{+}$ (**2**), with O_2 in the presence of HClO$_4$ to afford the hydroperoxo complex $[Cu^{II}(tepa)(OOH)]^{+}$ (**3**) via the formation of $[Cu^{II}(tepa)(O_2^{\bullet-})]^{+}$, followed by PCET reduction. The fast direct protonation of **3** with HClO$_4$ rather than electron-transfer reduction of **3** by Me$_2$Fc and Fc yields H$_2$O$_2$, accompanied by regenation of **1**, leading to the overall catalytic two-electron reduction of O_2 by Me$_2$Fc and Fc with HClO$_4$. The O_2 binding step to $[Cu^{I}(tepa)]^{+}$ combined with the PCET reduction of $[Cu^{II}(tepa)(O_2^{\bullet-})]^{+}$ with HClO$_4$ is the rate-limiting step in the overall catalytic reaction. The $-\Delta H$

Scheme 3
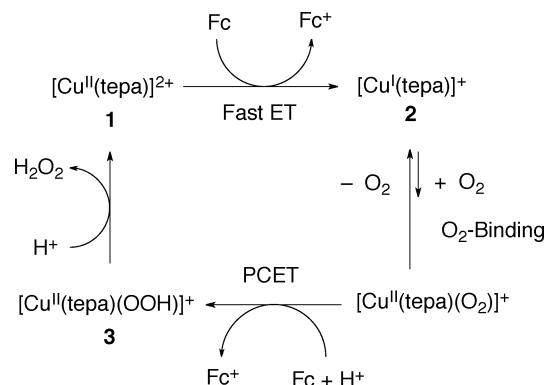
value of formation of $[Cu^{II}(tepa)(O_2^{\bullet-})]^+$ is very close to being the same as the $\Delta H^{\ddagger}$ value of the PCET reduction of $[Cu^{II}(tepa)(O_2^{\bullet-})]^+$, resulting in unique temperature-independent catalytic two-electron reduction of O_2 by weak one-electron reductants such as Me_2Fc and Fc in the presence of $HClO_4$ in acetone.

CONCLUSION

In summary, we have demonstrated that a subtle difference in ligand architecture, the addition if one $-CH_2-$ (methylene group) in the pyridylalkyl moiety of the ligand for Cu^{II} in $[Cu^{II}(tepa)]^{2+}$, as compared with chemistry carried out with $[Cu^{II}(tmpa)]^{2+}$, results in a drastic change in the number of electrons reacting in the catalytic reduction of O_2, a change from four for $[Cu^{II}(tmpa)]^{2+}$ to two for $[Cu^{II}(tepa)]^{2+}$. The more positive one-electron-reduction potential of $[Cu^{II}(tepa)]^{2+}$, in contrast to $[Cu^{II}(tmpa)]^{2+}$, has allowed us to employ relatively weak one-electron reductants, such as Fc and Me_2Fc, differing from the case of $[Cu^{II}(tmpa)]^{2+}$, which required the use of a strong one-electron reductant such as Fc^*. As a consequence, the rate-determining step changed from the electron-transfer reduction of $[Cu^{II}(tmpa)]^{2+}$ to its copper(I) form, to PCET reduction of $[Cu^{II}(tepa)(O_2^{\bullet-})]^+$ to form $[Cu^{II}(tepa)(OOH)]^+$, This latter process exhibits no temperature dependence, due to the cancellation of the heat of formation for the formation of $[Cu^{II}(tepa)(O_2^{\bullet-})]^+$ (a negative value) by the subsequent activation enthalpy for the PCET reduction (a positive value). It is also notable that, by use of perchloric acid to help drive the reaction toward Cu(II)−hydroperoxo formation, we have turned a copper(I) complex which is completely unreactive toward O_2 to undergo oxygenation and facilitation of catalytic O_2-reduction chemistry. This study has provided a deeper insight into the control of two-electron vs four-electron reduction of O_2, paving a promising way to the future development of efficient catalytic systems for production of H_2O_2, a promising candidate as a renewable energy source.[58,59]

ASSOCIATED CONTENT

Ⓢ Supporting Information

Kinetic analyses (Figures S1−S19). This material is available free of charge via the Internet at http://pubs.acs.org.

AUTHOR INFORMATION

Corresponding Author

*fukuzumi@chem.eng.osaka-u.ac.jp; karlin@jhu.edu; wwnam@ewha.ac.kr

REFERENCES

(1) (a) Holm, R. H.; Kennepohl, P.; Solomon, E. I. *Chem. Rev.* **1996**, *96*, 2239−2314. (b) Klinman, J. P. *Chem. Rev.* **1996**, *96*, 2541−2561. (c) Mirica, L. M.; Ottenwaelder, X.; Stack, T. D. T. *Chem. Rev.* **2004**, *104*, 1013−1046. (d) Lewis, E. A.; Tolman, W. B. *Chem. Rev.* **2004**, *104*, 1047−1076.

(2) (a) Solomon, E. I.; Ginsbach, J. W.; Heppner, D. E.; Kieber-Emmons, M. T.; Kjaergaard, C. H.; Smeets, P. J.; Tian, L.; Woertink, J. S. *Faraday Discuss.* **2011**, *148*, 11−39. (b) Solomon, E. I.; Sundaram, U. M.; Machonkin, T. E. *Chem. Rev.* **1996**, *96*, 2563−2605. (c) Solomon, E. I.; Chen, P.; Metz, M.; Lee, S.-K.; Palmer, A. E. *Angew. Chem., Int. Ed.* **2001**, *40*, 4570−4590. (d) *Bioinorganic Chemistry of Copper*; Karlin, K. D., Tyeklár, Z., Eds.; Chapman & Hall: New York, 1993. (e) Karlin, K. D.; Zuberbühler, A. D. Formation, Structure and Reactivity of Copper Dioxygen Complexes. In *Bioinorganic Catalysis*, 2nd ed.; Reedijk, J., Bouwman, E., Eds.; Marcel Dekker: New York, 1999; pp 469−534. (f) Quant Hatcher, L.; Karlin, K. D. *J. Biol. Inorg. Chem.* **2004**, *9*, 669−683. (g) Lee, Y.; Karlin, K. D. Highlights of Copper Protein Active-Site Structure/Reactivity and Synthetic Model Studies. In *Concepts and Models in Bioinorganic Chemistry*; Metzler-Nolte, N., Kraatz, H.-B., Eds.; Wiley-VCH: New York, 2006; pp 363−395.

(3) (a) Karlin, K. D. *Science* **1993**, *261*, 701−708. (b) Metzler-Nolte, N.; Kraatz, H.-B. *Concepts and Models in Bioinorganic Chemistry*; Wiley-VCH: New York, 2006.

(4) (a) Klinman, J. P. *J. Biol. Chem.* **2006**, *281*, 3013−3016. (b) Prigge, S. T.; Eipper, B.; Mains, R.; Amzel, L. M. *Science* **2004**, *304*, 864−867. (c) Chen, P.; Solomon, E. I. *Proc. Natl. Acad. Sci. U.S.A.* **2004**, *101*, 13105−13110. (d) Balasubramanian, R.; Smith, S. M.; Rawat, S.; Yatsunyk, L. A.; Stemmler, T. L.; Rosenzweig, A. C. *Nature* **2010**, *465*, 115−119. (e) Chan, S. I.; Yu, S. S.-F. *Acc. Chem. Res.* **2008**, *41*, 969−979.

(5) Humphreys, K. J.; Mirica, L. M.; Wang, Y.; Klinman, J. P. *J. Am. Chem. Soc.* **2009**, *131*, 4657−4663.

(6) Mukherjee, A.; Smirnov, V. V.; Lanci, M. P.; Brown, D. E.; Shepard, E. M.; Dooley, D. M.; Roth, J. P. *J. Am. Chem. Soc.* **2008**, *130*, 9459−9473.

(7) McGuirl, M. A.; Dooley, D. M. Copper Proteins with Type 2 Sites. In *Encyclopedia of Inorganic Chemistry*, 2nd ed.; King, R. B., Ed.; Wiley: Chichester, U.K., 2005; Vol. *II*, pp 1201−1225.

(8) (a) Blanford, C. F.; Heath, R. S.; Armstrong, F. A. *Chem. Commun.* **2007**, 1710. (b) Mano, N.; Soukharev, V.; Heller, A. *J. Phys. Chem. B* **2006**, *110*, 11180−11187.

(9) (a) Ferguson-Miller, S.; Babcock, G. T. *Chem. Rev.* **1996**, *96*, 2889−2908. (b) Pereira, M. M.; Santana, M.; Teixeira, M. *Biochim. Biophys. Acta* **2001**, *1505*, 185−208.

(10) (a) Tsukihara, T.; Aoyama, H.; Yamashita, E.; Tomizaki, T.; Yamaguchi, H.; Shinzawa-Itoh, K.; Nakashima, R.; Yaono, R.; Yoshikawa, S. *Science* **1995**, *269*, 1069−1074. (b) Yoshikawa, S.; Shinzawa-Itoh, K.; Nakashima, R.; Yaono, R.; Yamashita, E.; Inoue, N.; Yao, M.; Fei, M. J.; Libeu, C. P.; Mizushima, T.; Yamaguchi, H.; Tomizaki, T.; Tsukihara, T. *Science* **1998**, *280*, 1723−1729.

(11) (a) Collman, J. P.; Devaraj, N. K.; Decreau, R. A.; Yang, Y.; Yan, Y.-L.; Ebina, W.; Eberspacher, T. A.; Chidsey, C. E. D. *Science* **2007**, *315*, 1565−1568. (b) Collman, J. P.; Decreau, R. A.; Lin, H.; Hosseini, A.; Yang, Y.; Dey, A.; Eberspacher, T. A. *Proc. Natl. Acad. Sci. U.S.A.*

2009, *106*, 7320−7323. (c) Collman, J. P.; Ghosh, S.; Dey, A.; Decréau, R. A.; Yang, Y. *J. Am. Chem. Soc.* **2009**, *131*, 5034−5035.

(12) Kadish, K. M.; Frémond, L.; Shen, J.; Chen, P.; Ohkubo, K.; Fukuzumi, S.; El Ojaimi, M.; Gros, C. P.; Barbe, J.-M.; Guilard, R. *Inorg. Chem.* **2009**, *48*, 2571−2582.

(13) (a) Hatay, I.; Su, B.; Li, F.; Méndez, M. A.; Khoury, T.; Gros, C. P.; Barbe, J.-M.; Ersoz, M.; Samec, Z.; Girault, H. H. *J. Am. Chem. Soc.* **2009**, *131*, 13453−13459. (b) Partovi-Nia, R.; Su, B.; Li, F.; Gros, C. P.; Barbe, J.-M.; Samec, Z.; Girault, H. H. *Chem. Eur. J.* **2009**, *15*, 2335−2340. (c) Hatay, I.; Su, B.; Méndez, M. A.; Corminboeuf, C.; Khoury, T.; Gros, C. P.; Bourdillon, M.; Meyer, M.; Barbe, J.-M.; Ersoz, M.; Zális, S.; Samec, Z.; Girault, H. H. *J. Am. Chem. Soc.* **2010**, *132*, 13733−13741.

(14) (a) Partovi-Nia, R.; Su, B.; Méndez, M. A.; Habermeyer, B.; Gros, C. P.; Barbe, J.-M.; Samec, Z.; Girault, H. H. *ChemPhysChem* **2010**, *11*, 2979−2984. (b) Su, B.; Hatay, I.; Trojánek, A.; Samec, Z.; Khoury, T.; Gros, C. P.; Barbe, J.-M.; Daina, A.; Carrupt, P.-A.; Girault, H. H. *J. Am. Chem. Soc.* **2010**, *132*, 2655−2662.

(15) Zagal, J. H.; Griveau, S.; Silva, J. F.; Nyokong, T.; Bedioui, F. *Coord. Chem. Rev.* **2010**, *254*, 2755−2791.

(16) Cracknell, J. A.; Vincent, K. A.; Armstrong, F. A. *Chem. Rev.* **2008**, *108*, 2439−2461.

(17) (a) Thorum, M. S.; Yadav, J.; Gewirth, A. A. *Angew. Chem., Int. Ed.* **2009**, *48*, 165−167. (b) Thorseth, M. A.; Letko, C. S.; Rauchfuss, T. B.; Gewirth, A. A. *Inorg. Chem.* **2011**, *50*, 6158−6162. (c) McCrory, C. C. L.; Devadoss, A.; Ottenwaelder, X.; Lowe, R. D.; Stack, T. D. P.; Chidsey, C. E. D. *J. Am. Chem. Soc.* **2011**, *133*, 3696−3699. (d) Thorseth, M. A.; Tornow, C. E.; Tse, E. C. M.; Gewirth, A. A. *Coord. Chem. Rev.* **2013**, *257*, 130−139.

(18) (a) Stambouli, A. B.; Traversa, E. *Renew. Sust. Energy Rev.* **2002**, *6*, 295−304. (b) Marković, N. M.; Schmidt, T. J.; Stamenković, V.; Ross, P. N. *Fuel Cells* **2001**, *1*, 105−116. (c) Steele, B. C. H.; Heinzel, A. *Nature* **2001**, *414*, 345−352.

(19) Borup, R.; Meyers, J.; Pivovar, B.; Kim, Y. S.; Mukundan, R.; Garland, N.; Myers, D.; Wilson, M.; Garzon, F.; Wood, D.; Zelenay, P.; More, K.; Stroh, K.; Zawodzinski, T.; Boncella, J.; McGrath, J. E.; Inaba, M.; Miyatake, K.; Hori, M.; Ota, K.; Ogumi, Z.; Miyata, S.; Nishikata, A.; Siroma, Z.; Uchimoto, Y.; Yasuda, K.; Kimijima, K.-i.; Iwashita, N. *Chem. Rev.* **2007**, *107*, 3904−3951.

(20) (a) Lee, K.; Zhang, L.; Zhang, J. In *PEM Fuel Cell Electrocatalysts and Catalyst Layers*; Springer: London, 2008; p 715. (b) Anson, F. C.; Shi, C.; Steiger, B. *Acc. Chem. Res.* **1997**, *30*, 437−444. (c) Wang, B. *J. Power Sources* **2005**, 152. (d) Peljo, P.; Rauhala, T.; Murtomäki, L.; Kallio, T.; Kontturi, K. *Int. J. Hydrogen Energy* **2011**, *36*, 10033−10043.

(21) (a) Collman, J. P.; Devaraj, N. K.; Decréau, R. A; Yang, Y.; Yan, Y.-L.; Ebina, W.; Eberspacher, T. A; Chidsey, C. E. D. *Science* **2007**, *315*, 1565−1568. (b) Collman, J. P.; Decréau, R. A.; Lin, H.; Hosseini, A.; Yang, Y.; Dey, A.; Eberspacher, T. A. *Proc. Natl. Acad. Sci. U.S.A.* **2009**, *106*, 7320−7323. (c) Collman, J. P.; Ghosh, S.; Dey, A.; Decréau, R. A.; Yang, Y. *J. Am. Chem. Soc.* **2009**, *131*, 5034−5035.

(22) (a) Kadish, K. M.; Shen, J.; Frémond, L.; Chen, P.; Ojaimi, M. E.; Chkounda, M.; Gros, C. P.; Barbe, J.-M.; Ohkubo, K.; Fukuzumi, S.; Guilard, R. *Inorg. Chem.* **2008**, *47*, 6726−6737. (b) Chen, W.; Akhigbe, J.; Brückner, C.; Li, C. M.; Lei, Y. *J. Phys. Chem. C* **2010**, *114*, 8633−8645.

(23) (a) Rosenthal, J.; Nocera, D. G. *Acc. Chem. Res.* **2007**, *40*, 543−553. (b) Chang, C. J.; Loh, Z.-H.; Shi, C.; Anson, F. C.; Nocera, D. G. *J. Am. Chem. Soc.* **2004**, *126*, 10013−10020. (c) Dogutan, D. K.; Stoian, S. A; McGuire, R.; Schwalbe, M.; Teets, T. S.; Nocera, D. G. *J. Am. Chem. Soc.* **2011**, *133*, 131−140. (d) Teets, T. S.; Cook, T. R.; McCarthy, B. D.; Nocera, D. G. *J. Am. Chem. Soc.* **2011**, *133*, 8114−8117.

(24) (a) Fukuzumi, S.; Kotani, H.; Lucas, H. R.; Doi, K.; Suenobu, T.; Peterson, R. L.; Karlin, K. D. *J. Am. Chem. Soc.* **2010**, *132*, 6874−6875. (b) Tahsini, L.; Kotani, H.; Lee, Y.-M.; Cho, J.; Nam, W.; Karlin, K. D.; Fukuzumi, S. *Chem. Eur. J.* **2012**, *18*, 1084−1093.

(25) Halime, Z.; Kotani, H.; Li, Y.; Fukuzumi, S.; Karlin, K. D. *Proc. Natl. Acad. Sci. U.S.A.* **2011**, *108*, 13990−13994.

(26) Fukuzumi, S.; Tahsini, L.; Lee, Y.-M.; Ohkubo, K.; Nam, W.; Karlin, K. D. *J. Am. Chem. Soc.* **2012**, *134*, 7025−7035.

(27) (a) Yamada, Y.; Fukunishi, Y.; Yamazaki, S.-i.; Fukuzumi, S. *Chem. Commun.* **2010**, *46*, 7334−7336. (b) Jing, X.; Cao, D. X.; Liu, Y.; Wang, G. L.; Yin, J. L.; Wen, Q.; Gao, Y. Y. *J. Electroanal. Chem.* **2011**, *658*, 46−51.

(28) (a) Lei, T.; Tian, Y. M.; Wang, G. L.; Yin, J. L.; Gao, Y. Y.; Wen, Q.; Cao, D. X. *Fuel Cells* **2011**, *11*, 431−435. (b) Hasvold, O.; Storkersen, N. J.; Forseth, S.; Lian, T. J. *Power Sources* **2006**, *162*, 935−942. (c) Patrissi, C. J.; Bessette, R. R.; Kim, Y. K.; Schumacher, C. R. *J. Electrochem. Soc.* **2008**, *155*, B558−B562.

(29) (a) Disselkamp, R. S. *Energy Fuels* **2008**, *22*, 2771−2774. (b) Disselkamp, R. S. *Int. J. Hydrogen Energy* **2010**, *35*, 1049−1053.

(30) Galbács, Z. M.; Csányi, L. J. *J. Chem. Soc., Dalton Trans.* **1983**, 2353−2357.

(31) Latimer, W. M. *The Oxidation States of the Elements and their Potentials in Aqueous Solutions*; Prentice-Hall: New York, 1952; p 39.

(32) (a) Abrantes, S.; Amaral, E.; Costa, A. P.; Shatalov, A. A.; Duarte, A. P. *Ind. Crop. Prod.* **2007**, *25*, 288−293. (b) Zeronian, S. H.; Inglesby, M. K. *Cellulose* **1995**, *2*, 265−272.

(33) Li, L.; Lee, S.; Lee, H. L.; Youn, H. J. *BioResources* **2011**, *6*, 721−736.

(34) (a) Schatz, M.; Becker, M.; Thaler, F.; Hampel, F.; Schindler, S.; Jacobson, R. R.; Tyeklár, Z.; Murthy, N. N.; Ghosh, P.; Chen, Q.; Zubieta, J.; Karlin, K. D. *Inorg. Chem.* **2001**, *40*, 2312−2322. (b) Wei, N.; Murthy, N. N.; Karlin, K. D. *Inorg. Chem.* **1994**, *33*, 6093−6100.

(35) Armarego, W. L. F.; Chai, C. L. L. *Purification of Laboratory Chemicals*, 5th ed.; Butterworth-Heinemann: Amsterdam, 2003.

(36) Baek, H. K.; Karlin, K. D.; Holwerda, R. A. *Inorg. Chem.* **1986**, *25*, 2347−2349.

(37) Fukuzumi, S.; Ishikawa, M.; Tanaka, T. *J. Chem. Soc., Perkin Trans. 2* **1989**, 1037−1045.

(38) (a) Mair, R. D.; Graupner, A. J. *Anal. Chem.* **1964**, *36*, 194−203. (b) Fukuzumi, S.; Kuroda, S.; Tanaka, T. *J. Am. Chem. Soc.* **1985**, *107*, 3020−3027.

(39) (a) Karlin, K. D.; Hayes, J. C.; Juen, S.; Hutchinson, J. P.; Zubieta, J. *Inorg. Chem.* **1982**, *21*, 4106−4108. (b) Karlin, K. D.; Sherman, S. E. *Inorg. Chim. Acta* **1982**, *65*, L39−L40. (c) Ambundo, E. A.; Deydier, M.-V.; Grall, A. J.; Aguera-Vega, N.; Dressel, L. T.; Cooper, T. H.; Heeg, M. J.; Ochrymowycz, L. A.; Rorabacher, D. B. *Inorg. Chem.* **1999**, *38*, 4233−4242. (d) Rorabacher, D. B. *Chem. Rev.* **2004**, *104*, 651−697.

(40) (a) Lee, Y.-M.; Kotani, H.; Suenobu, T.; Nam, W.; Fukuzumi, S. *J. Am. Chem. Soc.* **2008**, *130*, 434−435. (b) Fukuzumi, S.; Kotani, H.; Prokop, K. A.; Goldberg, D. P. *J. Am. Chem. Soc.* **2011**, *133*, 1859−1869. (c) Fukuzumi, S.; Kotani, H.; Suenobu, T.; Hong, S.; Lee, Y.-M.; Nam, W. *Chem. Eur. J.* **2010**, *16*, 354−361. (d) Comba, P.; Fukuzumi, S.; Kotani, H.; Wunderlich, S. *Angew. Chem., Int. Ed.* **2010**, *49*, 2622−2625.

(41) The E_{ox} values of ferrocene derivatives in acetone are virtually the same as those in MeCN; see: Noviandri, I.; Brown, K. N.; Fleming, D. S.; Gulyas, P. T.; Lay, P. A.; Masters, A. F.; Phillips, L. *J. Phys. Chem. B* **1999**, *103*, 6713−6722.

(42) The activation entropy for electron transfer becomes negative when the electron transfer occurs via an intermediate; see: Fukuzumi, S.; Endo, Y.; Imahori, H. *J. Am. Chem. Soc.* **2002**, *124*, 10974−10975.

(43) Fujii, T.; Naito, A.; Yamaguchi, S.; Wada, A.; Funahashi, Y.; Jitsukawa, K.; Nagatomo, S.; Kitagawa, T.; Masuda, H. *Chem. Commun.* **2003**, 2700−2701.

(44) Wada, A.; Harata, M.; Hasegawa, K.; Jitsukawa, K.; Masuda, H.; Mukai, M.; Kitagawa, T.; Einaga, H. *Angew. Chem., Int. Ed.* **1998**, *37*, 798−800.

(45) Kodera, M.; Kita, T.; Miura, I.; Nakayama, N.; Kawata, T.; Kano, K.; Hirota, S. *J. Am. Chem. Soc.* **2001**, *123*, 7715−7716.

(46) (a) Karlin, K. D.; Cruse, R. W.; Gultneh, Y. *J. Chem. Soc., Chem. Commun.* **1987**, 599−600. (b) Karlin, K. D.; Ghosh, P.; Cruse, R. W.; Farooq, A.; Gultneh, Y.; Jacobson, R. R.; Blackburn, N. J.; Strange, R. W.; Zubieta, J. *J. Am. Chem. Soc.* **1988**, *110*, 6769−6780. (c) Root, D.

2833

dx.doi.org/10.1021/ja312523u | *J. Am. Chem. Soc.* 2013, 135, 2825−2834

E.; Mahroof-Tahir, M.; Karlin, K. D.; Solomon, E. I. *Inorg. Chem.* **1998**, *37*, 4838−4848.

(47) Kunishita, A.; Kubo, M.; Ishimaru, H.; Ogura, T.; Sugimoto, H.; Itoh, S. *Inorg. Chem.* **2008**, *47*, 12032−12039.

(48) In the case of $[Cu(tepa)]^{2+}$, $g_{xx} = g_{yy}$ with the same broad line width ($\sigma_{xx} = \sigma_{yy} = 100$ G). In such a case no superhyperfine due to nitrogens was detected. In the case of $[Cu^{II}(tepa)OOH]^+$, however, the line width of σ_{xx} (10 G) is much smaller than that of σ_{yy} (70 G) although $g_{xx} = g_{yy}$. This is the reason the superhyperfine due to nitrogens was detected for $[Cu^{II}(tepa)OOH]^+$ in Figure 8b,c.

(49) Alilou, E. H.; Hallaoui, A. E.; Ghadraoui, E. H. E.; Giorgi, M.; Pierrot, M.; Réglier, M. *Acta Crystallogr., Sect. C* **1997**, *C53*, 559−562.

(50) Karlin, K. D.; Hayes, J. C.; Hutchinson, J. P.; Hyde, J. R.; Zubieta, J. *Inorg. Chim. Acta* **1982**, *64*, L219−L220.

(51) Karlin, K. D.; Wei, N.; Jung, B.; Kaderli, S.; Niklaus, P.; Zuberbühler, A. D. *J. Am. Chem. Soc.* **1993**, *115*, 9506−9514.

(52) Karlin, K. D.; Kaderli, S.; Zuberbühler, A. D. *Acc. Chem. Res.* **1997**, *30*, 139−147.

(53) (a) Fukuzumi, S.; Endo, Y.; Imahori, H. *J. Am. Chem. Soc.* **2002**, *124*, 10974−10975. (b) Yoder, J. C.; Roth, J. P.; Gussenhoven, E. M.; Larsen, A. S.; Mayer, J. M. *J. Am. Chem. Soc.* **2003**, *125*, 2629−2640.

(54) (a) Zaman, K. M.; Yamamoto, S.; Nishimura, N.; Maruta, J.; Fukuzumi, S. *J. Am. Chem. Soc.* **1994**, *116*, 12099−12100. (b) Fukuzumi, S.; Ohkubo, K.; Tokuda, Y.; Suenobu, T. *J. Am. Chem. Soc.* **2000**, *122*, 4286−4294. (c) Zhu, X.-Q.; Zhang, J.-Y.; Cheng, J.-P. *J. Org. Chem.* **2006**, *71*, 7007−7015.

(55) Ohkubo, K.; Fukuzumi, S. *J. Phys. Chem. A* **2005**, *109*, 1105−1113.

(56) Zhang, C. X.; Kaderli, S.; Costas, M.; Kim, E.-i.; Neuhold, Y.-M.; Karlin, K. D.; Zuberbuhler, A. D. *Inorg. Chem.* **2003**, *42*, 1807−1824.

(57) Because the overall catalytic reaction has no temperature dependence, the $\Delta H^{\ddagger}$ value may be smaller than the $-\Delta H$ value of formation of the hydroperoxo complex in Scheme 2.

(58) Fukuzumi, S.; Yamada, Y.; Karlin, K. D. *Electrochim. Acta* **2012**, *82*, 493−511.

(59) (a) Yamada, Y.; Yoshida, S.; Honda, T.; Fukuzumi, S. *Energy Environ. Sci.* **2011**, *4*, 2822−2825. (b) Shaegh, S. A. M.; Nguyen, N.-T.; Ehteshami, S. M. M.; Chan, S. H. *Energy Environ. Sci.* **2012**, *5*, 8225−8228.